ISSN : 2350-0743

www.ijramr.com

International Journal of Recent Advances in Multidisciplinary Research
Vol. 06, Issue 03, pp.4765-4768, March, 2019

RESEARCH ARTICLE

STUDY ON MICROSTRUCTURE AND HARDNESS OF HEAT RESISTANT STEEL GIRTH WELD

***Yanan QIN and Yongyue YUAN**

Binzhou University, Binzhou, China

ARTICLE INFO

Article History:
Received 25th December, 2018
Received in revised form
20th January, 2019
Accepted 11th February, 2019
Published online 30th March, 2019

Keywords:
Heat resistant steel, Girth weld, Microstructure, Hardness.

****Corresponding author:*** **Yanan QIN**

ABSTRACT

The metallographic specimens of heat-resistant steel girth weld were prepared by cutting, inlaying, grinding, polishing and corrosion. The heat-affected zone, weld zone and base metal zone were observed and analyzed respectively. The results show that the structure of HAZ shows obvious coarse grains, and there exists Widmanstatten structure composed of cementite and pearlite in the superheated zone, and segregation occurs, which needs to be eliminated by post-weld heat treatment. Then the hardness of welds in different regions was tested by microhardness testing method. The results show that the micro hardness of different weld areas shows obvious difference.

INTRODUCTION

Metallographic analysis, as a traditional way of weld research, can effectively express the mechanical properties of weld, and has important significance in engineering (Dejun and Hai, 2018). Metallographic structure has good intuition, especially for weld, its morphology is affected by heat flux and moving speed of heat source. Therefore, the morphology characteristics of base metal, heat-affected zone and weld zone can be clearly distinguished, and the quality of weld process can be predicted and evaluated by judging and analyzing the morphology of the structure (Yongchuan and Kai, 2017). As a kind of chemical machinery material, heat-resistant steel needs higher welding temperature. The temperature variation of the weld during welding has a thermal cycling characteristic, which has a great influence on the residual stress of the weld and the morphology of the metallographic structure. In the prediction and judgment of weld mechanical properties, micro hardness is an advanced experimental method. The mechanical properties of welds in different directions can be obtained by statistical analysis of the hardness test data of welds in different directions and trajectories.

SAMPLE PREPARATION

Sample interception and mosaic: The metallographic analysis of the girth weld of heat-resistant steel mainly includes two parts: microstructure study and micro hardness test. The main object of analysis is the cross section of the welded joint. In order to ensure the reliability of the experiment, the electro spark wire-electrode cutting is used to cut the sample to avoid the secondary effect of thermal cutting on the weld structure. According to the symmetry of the circumferential weld, when the circumferential weld is cut, the central point of the circumferential weld is taken as the starting point and the circumferential weld is cut along the axial direction, and the cylindrical slice with the length of 20 mm is obtained. The slices contain the base metal zone, the weld zone and the heat affected zone of the weld. In order to facilitate the inlay of the sample, the cylindrical slice is cut into a fan-shaped slice with a central angle of 30 degrees along the radial direction (Zhiqiang, 2019). Axial cutting is carried out every 4 mm starting from the weld center of the slice. The model of mosaic machine used in the experiment is XQ-2B, and the mosaic method is thermal mosaic. The cross section of the mosaic finished sample is the analytic surface of the metallographic structure.

Sample grinding: After the metallographic specimens are inlaid, they need to be polished to obtain a bright surface. The main purpose of metallographic sample grinding is to prepare for polishing, which can be divided into two stages: rough grinding and fine grinding. Generally, the main tools used in rough grinding are file, milling machine, grinding machine, grinding wheel, etc. It can effectively eliminate the surface traces caused by sample cutting and the unevenness of weld surface. This step can be omitted if the surface of the sample itself is relatively flat or is cut by a tool with high accuracy (Chang, 2019). In order to ensure the safety of metallographic specimens in mechanical preparation and avoid the phenomenon that the specimens fly out or the sandpaper and polishing cloth are scratched due to uneven force in the process of grinding and polishing, it is necessary to grind the edges of mosaic specimens out of chamfer. The purpose of fine grinding is to eliminate some obvious scratches left in the preparation stage of rough grinding and prepare for more grinding (polishing). There are many different operation steps in the preparation stage of fine grinding, among which the most important one is the grinding step of metallographic sandpaper. Fine grinding operation mode has two kinds: manual grinding and mechanical grinding, which need to be completed manually by the experimenters. Fine grinding tools are usually gold sandpaper, which is composed of paper base, binder, and abrasive.

Polishing and corrosion: The first step of polishing is fine grinding, which aims at further eliminating the unevenness of the analyzed surface and making the surface a smooth mirror. Whether observed by naked eye or microscopy, they are polished marks. The polishing accuracy depends largely on the effect of the polishing process. Although only a thin layer of metal can be removed from the measured surface, it has a very important impact on the effect of metallographic preparation. At present, there are three main polishing methods: mechanical polishing, electrolytic polishing and chemical polishing. Among them, mechanical polishing is widely used by researchers because of its low cost and operation advantages. Mechanical polishing usually uses velvet cloth polishing, that means, the prepared polishing fluid droplets on or poured on the polishing cloth, and the polishing cloth rotates by mechanical rotation, so that the polishing fluid rubs against the surface of the sample, and the scratches on the surface of the sample after fine grinding are removed. The samples in this paper are polished by PG-1A polishing machine. After polishing, the samples need to be washed with water or alcohol for subsequent preparation process (Chang, 2019). There is no scratch on the surface of the sample with good polishing effect. It shows a bright surface under the optical microscope. Only by corrosion operation can the morphology of the metallographic structure be obtained. There are many kinds of metallographic corrosion methods, and according to the different materials of the sample, it is necessary to modulate the corrosion solution of different proportions. According to the material of the weld, chemical corrosion is adopted in this paper, which is also one of the most common corrosion modes. The corrosion was carried out by drip etching method. The corrosion solution was 4% nitric acid alcohol solution and the corrosion time was 15 seconds. After the corrosion was completed, the corrosion was washed with clean water immediately, then coated with anhydrous alcohol, and dried quickly with a blower. The specimens after corrosion will show obvious weld morphology (Yazhong, 2019). As shown in Fig. 1, it can be seen that due to the different grain boundary corrosion resistance, the annular welds show different morphologies and patterns after corrosion.

MICROSTRUCTURE ANALYSIS

Experimental condition: MM-10/10d optical metallographic microscope is selected as the microscope equipment, and the qualitative analysis of weld structure is completed by the metallographic analysis software of computer. The software is equipped with a professional quantitative metallographic image analysis system, which can evaluate the grain size of the analyzed object, especially the content of pearlite and ferrite, and input relevant statistical and analytical reports. The metallographic microscope has multistage magnification (Fei, 2018). In order to facilitate observation and analysis, the metallographic diagram of the weld is magnified about 400 times.

Base metal zone organization: As the base material, 30CrMoSi is a blank hot-rolled steel pipe after normalizing and tempering heat treatment. The microstructures of the base metal zone are shown in Fig.2 and Fig.3, including the non-phase transformation zone and part of the phase transformation zone. The shape of the particles is similar and the banded structure is obvious. The grains in black state are pearlite, while those in white state are ferrite. The size of grains varies, and the grains in some transformation zones are more refined.

Heat-affected zone structure: Because of the thinner thickness of the welded parts, the heat-affected zone (HAZ) is significantly affected by temperature. Fig.4 is a part of phase transformation zone in HAZ. On one side, the grain morphology of base metal can be seen. The structure is banded due to the influence of welding temperature. Small ferrite and pearlite grains increase in the phase transformation area, and the banded structure of the base metal gradually disappears, resulting in fine grains of black and white phase (Baoqiang, 2018). Far away from the weld zone, the temperature does not reach the austenite temperature, and the grain size in the zone does not change. With the effect of thermal cycling and austenitization occurs earlier in the weld zone with higher temperature, and the austenite nuclei appear between grains. When the welding process is completed, the temperature drops rapidly and small ferrite and pearlite are formed. When the temperature is higher than that of austenite and the holding time is long enough, a uniform pearlite and ferrite interphase particles will be formed. However, due to the short time at high temperature in the welding process, the grain size is relatively small, showing a banded structure.

The temperature range of this zone is controlled between Ac3 line and 1100 □ during welding. It is completely austenitized and the grain is refined. As shown in Fig.5, in the normalized zone of the middle part of the weld, the banded structure disappears and is replaced by a large number of uniform ferrite and pearlite particles, in which the ferrite and pearlite structure show interphase distribution characteristics. With the approach of welding zone, the temperature of HAZ metal increases further, the holding time is longer, and the grains grow gradually. As shown in Fig. 6, small particles grow from homogeneous grains in normalized zone to large grains. In the vicinity of the fusion zone, the temperature is high, the cooling speed is fast, and a large number of sorbite, bainite and ferrite are formed.

The welding area is in an overheated state because of the high temperature and the relatively long residence time at high temperature. The superheated structure formed after cooling consists of relatively large structure, as shown in Fig.7. Because of the segregation problem, there is a Widmanstatten structure containing cementite and pearlite in the superheated zone. Fig.8 shows the metallographic structure of the fusion zone. On the right is the weld zone, and near the fusion line is the semi-melting zone. As a hot spot, the heating temperature in the welding process is close to the melting point of the material. Because of the relatively long residence time at high temperature, the superheated structure formed by cooling has larger grains.

Microstructure of weld zone: There is obvious symmetrical distribution in the structure of the weld zone, and almost all the surface of the weld is superheated. According to the grain refinement of the weld surface, after a certain distance up and down, it gradually transits to a part of the normalized structure and phase transformation. Due to the rapid cooling rate of liquid metal in the weld during welding process, coarse grains appeared during recrystallization. As shown in Fig. 9, the typical weld structure is cylindrical ferrite and sorbite, which are hardly affected by other welding heat during welding. With the distance from the cover layer, the temperature is between Ac3 line and 1100 □, the austenitization is complete, the grain is refined, and after cooling, the uniform pearlite and ferrite particles are formed.

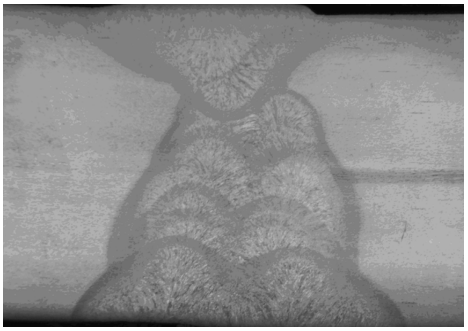

Fig.1 Corrosion effect of weld sample

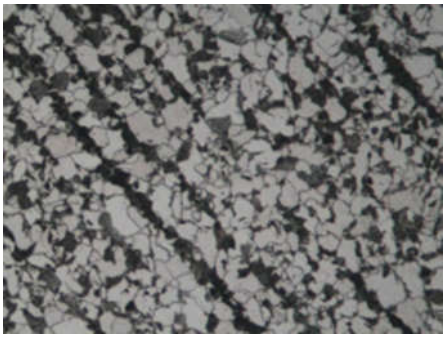

Fig.2 Microstructure of base metal

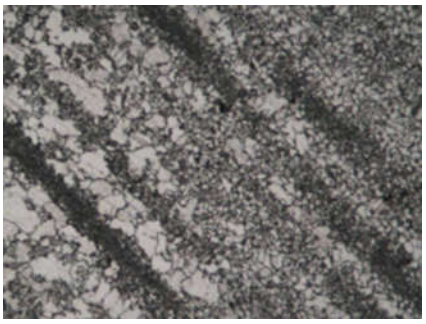

Fig.3 Partial Phase Change Zone of Base Material

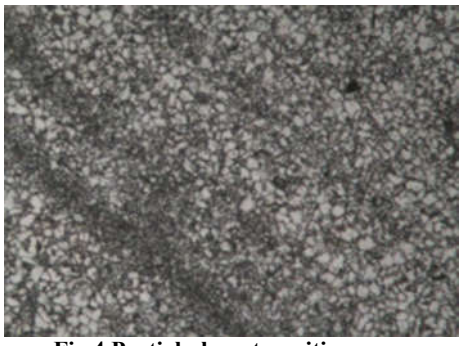

Fig.4 Partial phase transition zone

Fig.5 Normalizing zone

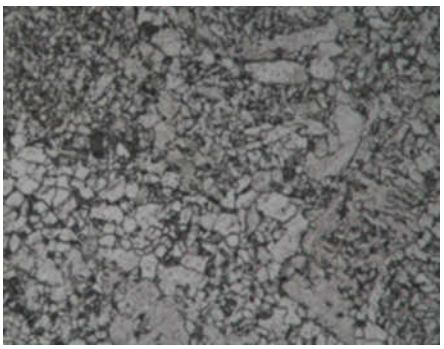

Fig.6 Overheated zone

Fig.7 Segregation structure in Overheated zone

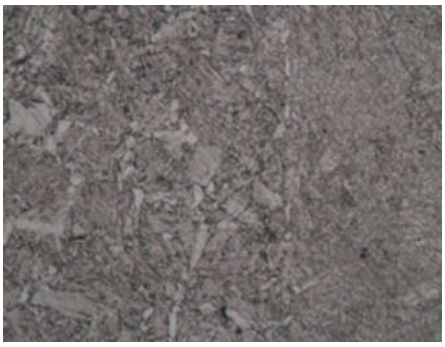

Fig.8 Microstructure of weld fusion zone

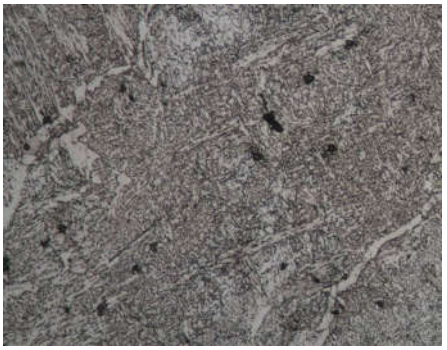

Fig.9 Microstructure of overlay on weld seam

MICROHARDNESS ANALYSIS

Experimental condition: The ability of hardness material to resist local deformation is also an important criterion to measure surface hardness and softness. Hardness can fully reflect the strength, plasticity, wear resistance and other properties of the material. It has less damage to the surface of the test sample and is more convenient and fast in a smaller measurement range. The hardness test is carried out by automatic micro hardness tester. The test is carried out according to the predetermined procedure, including test points, indentation forming, observation and measurement of indentation, which can form hardness data and output experiment report. Referring to the analysis results of the microstructure, several hardness lines in different directions were selected for testing, as shown in Fig. 10. Hardness lines of a, b, c and d hardness lines were taken horizontally for analysis. In the welding process, the fusion line is the demarcation line of the welding heat, and the hardness analysis of the fusion line and its two sides along the fusion line direction is more representative.

Hardness distribution analysis: The results of transverse hardness distribution is shown in Fig.11.

The hardness curve a is located in the upper cover, most of the sampling points are in the welding zone, and a few in the heat affected zone and the base metal zone.

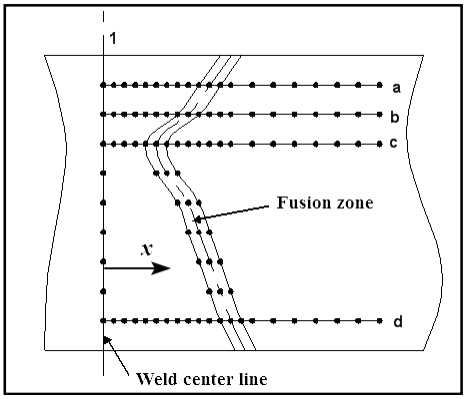

Fig. 10. Sampling point position of hardness

Curve b shows typical superheated structure in the welding zone, and its hardness is higher than that in the fusion zone. With entering the heat affected zone, the time to reach the maximum temperature decreases, and the structure has a certain holding time. Relatively fine structure makes hardness lower. Curve c expresses the structure of normalizing zone.

Because of the influence of welding heat, the temperature of some welding zones is higher than Ac3. Due to a certain holding time, the phase transformation is completed, the structure is normalized or part of the phase transformation zone and the relative hardness of the covered surface are lower. Curve d represents the internal weld layer. The welding process has many heating times and fast cooling speed. Its microstructure is columnar ferrite, sorbite and bainite, and its hardness is higher.

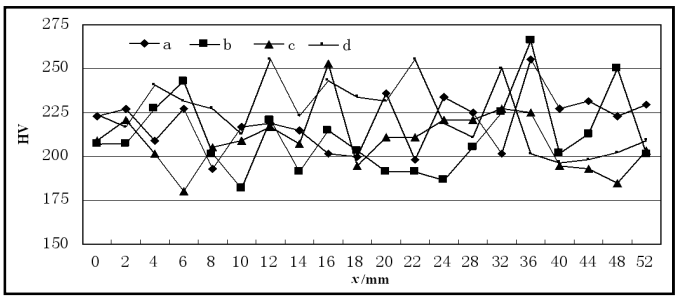

Fig.11 Transverse hardness distribution

Acknowledgement

The paper is supported by the Youth Talent Innovation Project (BZXYQNLG201703).

Conclusion

The experimental research includes microstructure analysis and microhardness test. The base material of the welded joint is 30CrMoSi, which has been normalized and tempered. In this paper, the metallographic samples of the girth weld were prepared by cutting and inserting, grinding, polishing and corrosion operations. Microstructure characteristics of weld were observed under metallographic microscope, and metallographic composition and formation reasons of base metal zone, heat-affected zone and weld zone were analyzed. The transverse and longitudinal hardness of the weld seam were tested by micro hardness tester, and the internal factors of the mechanical properties of the weld seam were obtained by analysis.

REFERENCES

Dejun, Y. and Hai, L. 2018. Microstructure and properties of variable polarity plasma welded joint of 5083 aluminum alloy for ship. *Rare Metal Materials and Engineering*, 47(02): 3161-3166.

Yongchuan, L. and Kai, W. 2017. Effect of Graphite Morphology and Metallographic Microstructure on Mechanical Properties of Vermicular Graphite Cast Iron. *Casting Technology*, 38(03): 2582-2585.

Zhiqiang, H. 2019. 12Cr1MoVG/T91 Dissimilar Steel Joint Crack Formation Reason Analysis. *Welding Technology*, 20(11): 76-80.

Chang, X. 2019. Fracture Failure Analysis of Connecting Bolts of Pump Body. *Mechanical Engineering and Automation*, 19(08): 143-144.

Yazhong, Z. 2019. Microstructure of high chromium cast iron from the perspective of composite materials. *Casting Technology*, 40(05): 156-160.

Fei, L. 2018. AlSi10Mg Aluminum Alloy Laser Melting Deposition Microstructure and Mechanical Properties. *Journal of South China University of Technology (Natural Science Edition)*,46(10):117-125.

Baoqiang, C. 2018. Microstructure and Properties of Dual Pulse VP-GTAW Joints for Aluminum Alloys. *Aviation Manufacturing Technology*, 61(02): 16-21.

****